PHYSICAL REVIEW B **84**, 140104(R) (2011)

Dense close-packed phase of tin above 157 GPa observed experimentally via angle-dispersive x-ray diffraction

Ashkan Salamat,[1,*] Gaston Garbarino,[1] Agnès Dewaele,[2] Pierre Bouvier,[3] Sylvain Petitgirard,[1] Chris J. Pickard,[4] Paul F. McMillan,[5] and Mohamed Mezouar[1]

[1]*European Synchrotron Radiation Facility, Boîte Postale 220, F-38043 Grenoble Cedex, France*

[2]*CEA, Bruyères-le-Châtel, F-91297 Arpajon Cedex, France*

[3]*Laboratoire des Matériaux et du Génie Physique, CNRS, Grenoble Institute of Technology, MINATEC, 3 Parvis Louis Néel, F-38016 Grenoble, France*

[4]*Department of Physics and Astronomy, University College London, Gower Street, London WC1E 6BT, United Kingdom*

[5]*Department of Chemistry and Materials Chemistry Centre, University College London, 20 Gordon Street, London WC1H 0AJ, United Kingdom*

(Received 6 July 2011; revised manuscript received 10 August 2011; published 31 October 2011)

A hexagonal close-packed ($P63/mmc$) phase of the group 14 element Sn has been observed using angle-dispersive x-ray diffraction. The phase transition proceeds from bcc → hcp above 157 GPa at 298 K via a first-order pathway, accompanied by a small decrease in unit-cell volume (0.2%). Both phases coexist up to 194 GPa. *Ab initio* random structure search calculations confirm that the hcp phase is the only candidate for another polymorph of Sn occurring in this pressure range, and predict a return to the bcc structure above 1.3 TPa.

DOI: 10.1103/PhysRevB.84.140104 PACS number(s): 62.50.−p, 61.66.Bi, 64.70.K−

All elements are expected to transform to fully dense metallic states at the highest pressures. However, experiments carried out into the megabar range ($P > 100$ GPa) combined with *ab initio* theory are leading to a deeper understanding of how electronic structure and atomic packing evolve at extremely high density.[1,2] Studies of *sp*-bonded metals and non-metallic systems such as Ba,[3] Rb,[4] and Se (Ref. 5) show complex structural behavior with disproportion occurring in the electron density, producing "elemental alloys" at high pressure. *Ab initio* compression studies extending into the TPa range, now accessible using laser shock facilities[6,7] and relevant to extrasolar planetary studies, reveal electride-like behavior among metals such as Al,[8] where the electron density becomes concentrated away from the atomic cores and bonding regions. Here we investigate the structural properties of elemental Sn into the multi-megabar domain and provide experimental evidence for a long-predicted hcp phase. We then predict re-entrant behavior of the bcc structure as electride-like properties appear in the TPa regime.

The group 14 elements (C, Si, Ge, Sn, Pb) straddle the boundary between semiconducting and insulating behavior. At ambient P, diamond-structured sp^3-bonded solids occur for Si and Ge that transform into dense metallic phases with six-fold to 12-fold coordination as the pressure is increased. Sn lies between these elements and Pb that is always metallic, and its pressure-induced phase transition properties help determine the role of *s-p-d* bonding as a function of density. At ambient conditions, it crystallizes with a metallic β-Sn structure containing the atoms in distorted octahedral coordination within a body-centered-tetragonal (bct) lattice. The diamond-structured α-Sn phase is stabilized at low T. Above 9.5 GPa the β-Sn phase is reported to transform into a further bct structure.[9] At 40 GPa reflections appear in the x-ray diffraction pattern that have been assigned to a bcc structure, and both bct and bcc phases apparently coexist over a wide pressure range up to 52 GPa.[10] This unusual behavior can be explained by multiple minima occurring in the potential energy surface at different c/a ratios.[11,12] These are correlated with unusual electronic behavior as *d*-level participation along with relativistic terms and spin-orbit coupling become important in the bonding.[13] As the applied pressure enters the megabar range ($P > 100$ GPa), the structure is predicted to achieve a bcc geometry as the minimum with $c/a = 1$ deepens and becomes dominant. As early as 1989 Desgreniers *et al.* proved the existence of the bcc phase up to 120 GPa using energy-dispersive x-ray diffraction.[14] Based on analogies with Si, Ge, and Pb, they suggested that a close-packed hcp phase should become stable under sufficiently high compression, but they noted difficulties with current theoretical methods to predict the critical atomic radii. These authors suggested that "first-principle total-energy calculations be re-examined for the possible existence of close-packed structures for tin at very high pressures."[14] Several such high-level calculations have now been carried out but have obtained widely different results.[15] Several studies suggested that no hcp phase should appear below 2 Mbar (200 GPa);[12,16] others have suggested bcc → hcp phase transition pressures as low as 61 GPa (Ref. 17) and 90 GPa.[18] None of these predictions have been supported by experiment.

We report the experimental observation of the bcc → hcp phase transition in Sn combining state-of-the-art synchrotron angle-dispersive x-ray diffraction techniques with quasi-hydrostatic loading in the diamond-anvil cell (DAC) to ∼2 Mbar. The experimental results are combined with an *ab initio* theoretical study using random structure searching techniques (AIRSS) and density functional theory (DFT) methods,[19] paying close attention to the convergence criteria. The results indicate why there has been such divergence among previous theoretical predictions of the high-pressure behavior of this element. Continuing the AIRSS investigation into the terapascal range reveals a different electronic structure and bonding behavior as the bcc form becomes re-entrant above 1.3 TPa.

Experiments were carried out using a membrane-driven DAC with the sample Sn (99.9%, Merck) loaded along with W (99.9%, Goodfellow) and SrB_4O_7:Sm^{2+} as pressure indicators.

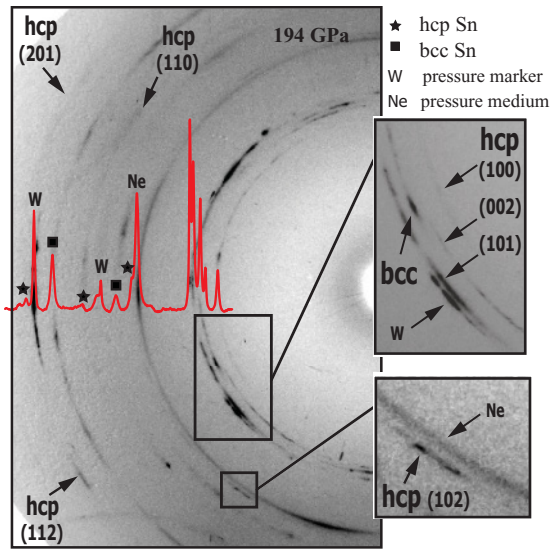

FIG. 1. (Color online) An image from the MarCCD at 194 GPa. The Debye-Scherrer diffraction rings due to the hcp phase of Sn are identified among the bcc Sn, W, and Ne phases. The integrated diffraction pattern is overlaid on the diffraction image.

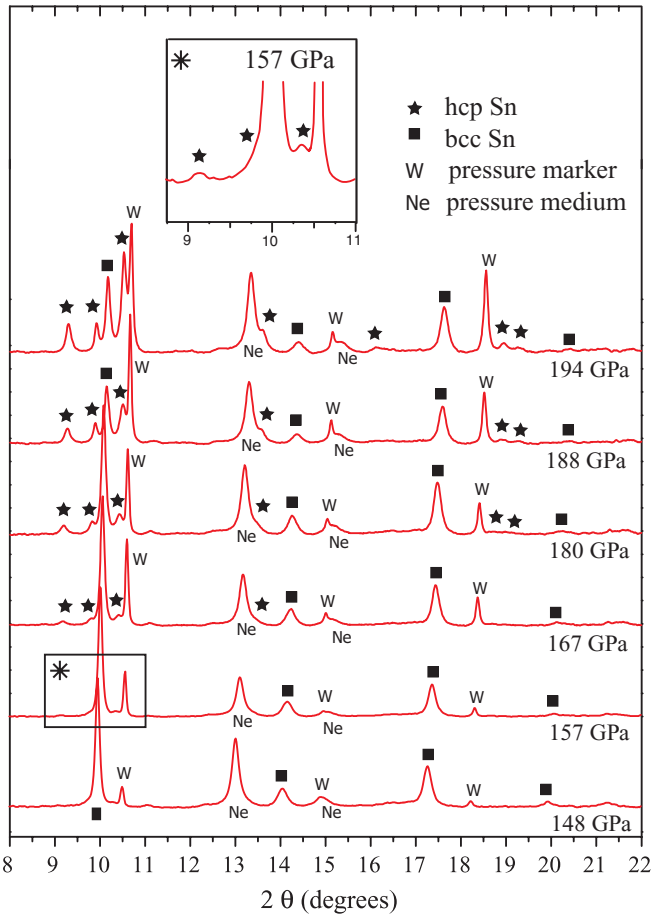

FIG. 2. (Color online) X-ray diffraction patterns ($\lambda = 0.3738$ Å) showing the compression of Sn from 148 to 194 GPa at room temperature. The hcp and bcc phases are marked by a solid star and square symbol, respectively. The tungsten pressure maker is represented by its chemical symbol W, as is the neon pressure transmitting medium, Ne. The asterisked box reveals a closeup of the diffraction pattern at 157 GPa showing the emergence of the 100, 002, and 101 reflections of the hcp phase.

The fluorescence marker was used to provide initial estimates of pressures in the sample chamber during the experiment,[20] but final pressures were determined using the Vinet equation of state (EOS) of W with $K_0 = 296$ GPa and $K_0' = 4.3$.[21] Two compression runs were conducted using 100- and 75-μm bevelled diamonds with He or Ne as pressure transmitting media (PTM). Maximum pressures attained in the two studies were 140 and 194 GPa. Re gaskets were drilled using a Nd:yttrium aluminum garnet (YAG) laser. Angle-dispersive synchrotron x-ray diffraction was carried out at beamline ID27 of the European Synchrotron Radiation Facility. A high-energy (33 keV, $\lambda = 0.3738$ Å) monochromatic beam was focused down to a full width at half maximum (FWHM) of 1.7×2.3 μm, enabling us to avoid diffraction lines from the gasket material potentially contaminating the pattern (Fig. 1). These technical features are vital for structural analysis of the data sets. Data were collected using a MarCCD 165 detector with 20–60 s exposure. *Ab initio* calculations were carried out with the Perdew-Burke-Ernzerhof generalized gradient approximation (GGA)[22] density functional using the plane-wave code in CASTEP.[23] The basis set cutoff energy was set to 359 eV using a 14-electron ultrasoft pseudopotential.[24] We defined a 2.3 a.u. core radius for the local and non-local channels and a value of 1.6 a.u for the cutoff radius for the pseudoionization of the augmentation charge. Different k-point sets were used with a $18 \times 18 \times 18$ Monkhorst-Pack (MP)[25] k-point grid for the conventional bcc cell, and $24 \times 24 \times 14$ for the hcp structure. These are larger grids with finer resolution than used in previous studies. We carried out *ab initio* random structure searching (AIRSS) runs[19,26] at 200 GPa and 2 TPa in cells with up to six atoms to investigate possible alternative structures as well as further evolution beyond the hcp phase at high density.

The first indication of hcp Sn occurs at 157 GPa with the emergence of the 100, 002, and 101 reflections of a hexagonal structure (Fig. 2). By 167 GPa sufficient reflections were available to identify $P63/mmc$ as the highest symmetry space group consistent with the systematic absences and to carry out a Rietveld analysis, leading to $a = 2.690(2)$ Å and $c = 4.375(5)$ Å [$V_p = 13.71(9)$ Å^3] with Sn atoms occupying the Wyckoff site $2c$ at $\frac{1}{3}, \frac{2}{3}, \frac{1}{4}$ (Fig. 3). The hcp phase shows a c/a ratio of 1.621(6), slightly smaller than the ideal value of 1.633; this ratio is maintained up to a maximum pressure (194 GPa) with $a = 2.662(5)$ Å and $c = 4.318(7)$ Å [$V_p = 13.25(7)$ Å^3].

The $V(P)$ relations of the hcp and bcc phases were evaluated using a finite strain Birch-Murnaghan EOS expanded to third order[27] (Fig. 4). Because neither polymorph is recoverable, the experimental EOS relations were evaluated relative to a reference volume specified at high pressure (V_p). Bulk modulus (K_p) and its pressure derivative (K_p') were determined by two procedures: first, fitting $V(P)$ assuming $K_p' = 4.0$ to return an initial estimate of K_p, then varying both parameters along with V_p. Theoretical EOS data were determined from the DFT energy-volume relations at $T = 0$ K. The hcp phase [$V_p = 13.96(6)$ Å^3] gave $K_p = 652(20)$ GPa assuming $K_p' = 4.0$, and $K_p = 604(14)$ GPa and $K_p' = 5.1(9)$

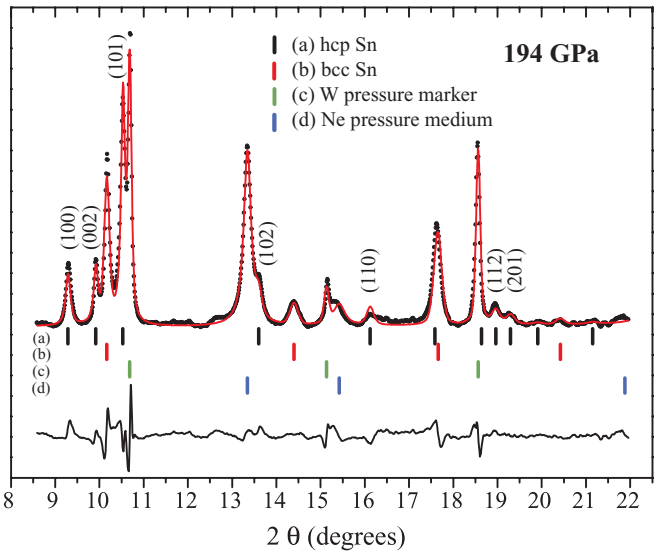

FIG. 3. (Color online) Rietveld refinement of the hcp and bcc phases of Sn and the W pressure marker in a Ne pressure medium at 194 GPa. The data points and the Rietveld fit are shown as black dots and a red line, respectively. The difference plot is shown underneath. The tick marks are representative of the four phases accounted for and are given as (a) hcp ($P63/mmc$) Sn, (b) bcc (Im-$3m$) Sn, (c) W (Im-$3m$), and (d) Ne (Fm-$3m$). The wR_p and R_p values are 1.99% and 1.52%, respectively.

at a reference $P = 157(4)$ GPa. These compare well with the theoretical prediction: $V_p = 14.16$ Å^3, $K_p = 626(1)$ GPa, $K_0' = 3.4(1)$ using $P = 157(5)$. The bcc EOS was derived from data obtained from He and Ne PTM runs with $V_p = 15.78(4)$ Å^3 and $K_p = 400(20)$ GPa, $K_p' = 3.3(7)$ at $P = 100(3)$. These again compare well with our theoretical predictions with V_p refined as 15.90 Å^3 and $K_p = 442(1)$ GPa, $K_p' = 3.6(1)$ at $P = 100(5)$ GPa.

The bcc → hcp transition results in a very small volume contrast of 0.21(4)% between the two phases that agrees with our calculated value predicted by DFT methods (0.13%) at $T = 0$ K. Calculated volumes were within 1.4% of the experimental values throughout the pressure range studied. We observed some small effects of non-hydrostatic strain between studies carried out with Ne versus He PTM loading. However, an error analysis of the experiments carried out up to 140 GPa for the bcc polymorph showed that such differences were negligible in a single-phase regime. Using Ne as PTM resulted in uncertainties in P determined from the W EOS of ±4 GPa increasing to a maximum possible ±6 GPa by 194 GPa while the He PTM above 100 GPa gave a pressure with a maximum uncertainty of ±3 GPa. However, examining the EOS of hcp and bcc phases from 157 to 194 GPa, we note a contribution from non-hydrostatic stress effects resulting from the metastable coexistence of the two phases that can be seen as a very slight deviation from the ideal EOS relations versus experimental or theoretical data fits (Fig. 4). Over this pressure range the calculated enthalpy difference between the two phases is only 5 meV/atom (∼1 kJ/mol). Added to the fact that they have very similar volumes, the observed coexistence over a large pressure range is consistent with the prediction.

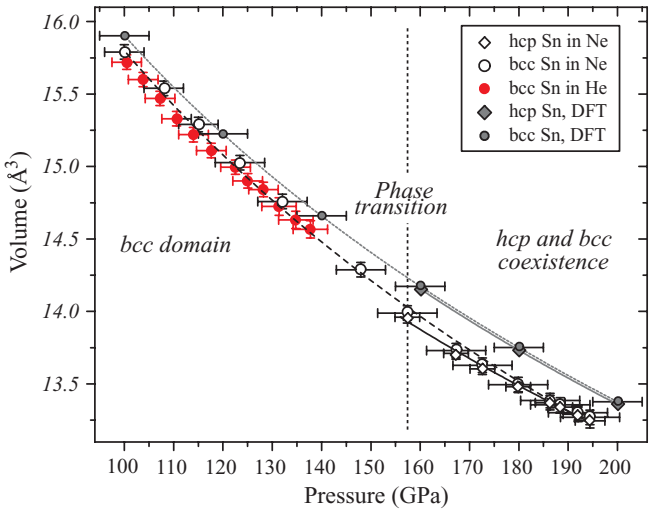

FIG. 4. (Color online) $V(P)$ plot of the experimental and theoretical results showing the hcp and bcc phases of Sn and their respective fits using a Birch-Murnaghan equation of state (EOS) expanded to third order. The experimental data sets are given for the Sn loaded in He and Ne pressure transmitting medium while the theoretical data for the two phases are marked as DFT. The experimental and theoretical hcp EOS fits are represented with black lines while the bcc phase is fitted with dashed lines.

Our theoretical calculations were found to be highly sensitive to convergence criteria with respect to the density of the k-point grid. Previous studies likely underestimated this sensitivity and found the relative stability of the hcp phase remained much too high with respect to the bcc phase, predicted the presence of additional polymorphs at high density, or lost essential precision in the predicted bcc → hcp transition pressure.[12,17] Having identified this as a main factor, we included large k-point sampling grids in our calculations, which represented an order-of-magnitude improvement over previous investigations.[16] It is worth pointing out that the theoretical calculations were carried out independently from

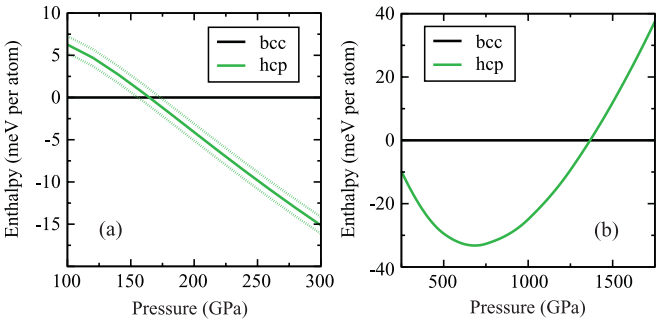

FIG. 5. (Color online) Enthalpy-pressure plots. The relative enthalpies (H) are for the hcp and bcc phases of Sn. (a) The $H(P)$ plot ranges from 100 to 300 GPa and shows the pressure-induced transition occurring at 160 GPa. The two dotted lines show the effects of shifting the relative enthalpies by 1 meV that causes a change in the predicted transition pressure of ∼10 GPa. This corresponds to a likely estimate of the maximum error in our calculations. We found no other candidate structures in this pressure range. (b) Continuing the $H(P)$ plot to higher pressures between 250 and 1750 GPa shows the bcc phase becomes re-entrant at ∼1300 GPa (1.3 TPa).

and with no prior knowledge of the experimental phase transition behavior. Figure 5 shows enthalpy (H)-pressure plots derived from our calculations. The dotted lines demonstrate the effects of shifting the relative enthalpies by 1 meV that would correspond to a change in transition pressure of 10 GPa: We estimate the accuracy of our calculations to be similar. The experimentally observed transition pressure of 157 GPa closely matches the value predicted by our DFT calculations, 160(5) GPa (at $T = 0$ K). We note that the previous work by Aguado[28] predicted a phase transition pressure of 163 GPa, and that the work carried out by Yu *et al*. also predicted an accurate transition pressure of 160 GPa to the hcp phase.[29]

Continuing the AIRSS and DFT studies to higher pressures within the terapascal range, we find that the bcc structured polymorph is likely to become re-entrant at $P > 1.3$ TPa (Fig. 5). That is an unexpected result that suggests a dramatic change in electronic behavior for this apparently simple group 14 element. An analysis of the electron density of this high-density bcc form indicates that clusters may be forming away from the atom centers and interatomic bonding regions, leading to an electride-like behavior, as previously described for Al in the TPa range.[8]

In summary, we present convincing experimental evidence for the existence of the hcp phase of Sn that has long been predicted to occur but never observed. We find a transition onset pressure of 157 GPa that corresponds very well with our *ab initio* calculation results. We observe very small volume and enthalpy changes associated with the first-order phase transition. The variability in previous theoretical predictions are identified as due to the extreme sensitivity to convergence with respect to dimensions and sampling of the k-point grid. Our calculations clearly identify the hcp phase as the stable polymorph at pressures above 160 GPa. Finally, we predict that the bcc structure becomes stable, once more above 1.3 TPa, as the electronic structure evolves toward electride-like behavior, with concentrations of electron density emerging away from the ion cores and conventional bonding regions.

The authors thank the ESRF for providing beamtime. We thank Paul Loubeyre and Florent Occelli for scientific input and experimental help. P.F.M. and C.J.P. are both supported by the EPSRC.

*ashkan.salamat@esrf.fr

[1] Y. Akahama, M. Nishimura, K. Kinoshita, H. Kawamura, and Y. Ohishi, Phys. Rev. Lett. **96**, 45505 (2006).
[2] X. J. Chen, C. Zhang, Y. Meng, R. Q. Zhang, H. Q. Lin, V. V. Struzhkin, and H. K. Mao, Phys. Rev. Lett. **106**, 135502 (2011).
[3] M. I. McMahon, O. Degtyareva, and R. J. Nelmes, Phys. Rev. Lett. **85**, 4896 (2000).
[4] R. J. Nelmes, M. I. McMahon, J. S. Loveday, and S. Rekhi, Phys. Rev. Lett. **88**, 155503 (2002).
[5] C. Hejny and M. I. McMahon, Phys. Rev. Lett. **91**, 215502 (2003).
[6] [http://lasers.llnl.gov/].
[7] D. K. Bradley, J. H. Eggert, R. F. Smith, S. T. Prisbrey, D. G. Hicks, D. G. Braun, J. Biener, A. V. Hamza, R. E. Rudd, and G. W. Collins, Phys. Rev. Lett. **102**, 75503 (2009).
[8] C. J. Pickard and R. J. Needs, Nat. Mater. **9**, 624 (2010).
[9] H. Olijnyk and W. B. Holzapfel, J. Phys. C **8-11**, 153 (1984).
[10] M. Liu and L. Liu, High Temp. High Press. **18**, 79 (1986).
[11] N. E. Christensen, Solid State Commun. **85**, 151 (1993).
[12] N. E. Christensen and M. Methfessel, Phys. Rev. B **48**, 5797 (1993).
[13] N. E. Christensen, S. Satpathy, and Z. Pawlowska, Phys. Rev. B **34**, 5977 (1986).
[14] S. Desgreniers, Y. K. Vohra, and A. L. Ruoff, Phys. Rev. B **39**, 10359 (1989).
[15] D. Mukherjee, K. D. Joshi, and S. C. Gupta, J. Phys.: Conf. Ser. **215**, 12106 (2010).
[16] S. X. Cui, L. C. Cai, W. X. Feng, H. Q. Hu, C. Z. Wang, and Y. X. Wang, Phys. Status Solidi B **245**, 53 (2008).
[17] B. H. Cheong and K. J. Chang, Phys. Rev. B **44**, 4103 (1991).
[18] J. L. Corkill, A. Garcia, and M. L. Cohen, Phys. Rev. B **43**, 9251 (1991).
[19] C. J. Pickard and R. J. Needs, J. Phys. Condens. Matter **23**, 53201 (2011).
[20] F. Datchi, R. LeToullec, and P. Loubeyre, J. Appl. Phys. **81**, 3333 (1997).
[21] A. Dewaele, P. Loubeyre, and M. Mezouar, Phys. Rev. B **70**, 94112 (2004).
[22] J. P. Perdew, K. Burke, and M. Ernzerhof, Phys. Rev. Lett. **77**, 3865 (1996).
[23] S. J. Clark, M. D. Segall, C. J. Pickard, P. J. Hasnip, M. J. Probert, K. Refson, and M. C. Payne, Z. Kristallogr. **220**, 567 (2005).
[24] D. Vanderbilt, Phys. Rev. B **41**, 7892 (1990).
[25] H. J. Monkhorst and J. D. Pack, Phys. Rev. B **13**, 5188 (1976).
[26] C. J. Pickard and R. J. Needs, Phys. Rev. Lett. **97**, 45504 (2006).
[27] F. Birch, Phys. Rev. **71**, 809 (1947).
[28] A. Aguado, Phys. Rev. B **67**, 212104 (2003).
[29] C. Yu, J. Y. Liu, H. Lu, and J. M. Chen, Solid State Commun. **140**, 538 (2006).